

**STRESS STATE AND DEFORMATION (STRAIN) ENERGY  
DISTRIBUTION AHEAD CRACK TIP  
IN A PLATE SUBJECTED TO TENSION**

*UDC 531:620.136:620.10*

**Dragan B. Jovanović**

Faculty of Mechanical Engineering, University of Niš

Beogradska 14, 18000 Niš

E-mail: jdragan@masfak.masfak.ni.ac.yu

**Abstract.** *Three-dimensional model of the plate, with the elliptical crack contour is used for analyzing of stress state and deformation energy, in this paper. It is assumed that tensile forces are applied at the direction perpendicular on the crack plane, and that stress state is two-dimensional in general (in remote regions). Three-dimensional stress state at the vicinity of crack front zone is evaluated by using of finite element method. Evidently, variation of stress tensor components is related to the coordinate perpendicular to the middle plane of the plate, and  $\sigma_z$  is different from zero at the region nearby around the crack.*

*In this paper obtained results on stress and deformation (strain) energy distribution are analyzed, and conclusions about the three-dimensional stress state and three-dimensional energy distribution in the region close to crack front line are obtained.*

**Key words:** *crack, stress state, specific deformation (strain) energy, reconstruction of deformation (strain) energy surfaces.*

## 1. INTRODUCTION, FRAMEWORK

The conventional plate theories assume that the stress variations in terms of the thickness coordinate are known a priori [14], [26], and [27]. For plane stress state, the transverse normal stress component  $\sigma_z$  is assumed to be zero throughout the plate, and in-plane stresses  $\sigma_x$ ,  $\sigma_y$  and  $\tau_{xy}$  are independent on thickness coordinate [1], [4], [15]. These assumptions are valid under very limited circumstances, and in the very narrow framework [22], [23], [27], and [28].

Three-dimensional model of the plate, with the crack of elliptical contour is accepted for the analysis. It is assumed that axial tensile forces are applied in direction perpendicular to the crack plane, and that general stress state in plate is two-dimensional. Three-dimensional stress state at the crack tip zone by using of finite element method is

evaluated. Evidently varying of stress tensor components is related to the coordinate perpendicular to the middle plane of the plate and  $\sigma_z$  is different from zero in the region around the crack.

Diagrams of stress components, in sections  $x=0$ ,  $y=0$  and  $z=0$  are presented. Strain energy for directions  $y=0$ ,  $z=0, \pm 1, \pm 2, \pm 3, \pm 4, \pm 5$  mm and  $z=0$ ,  $x=0, 2.3, 3.35, 4.5, 6.15, 7.03, 9.3, 10.76, 14.4, 20.93, 25, 30.32, 35, 40, 45, 48.5$  mm is calculated. Surface of the strain energy for points in the middle plane and plane perpendicular to it, in front of the crack tip, by using relations for strain energy, best fitting curve, best fitting surface, and iteration procedure is reconstructed. Variation of stress components and distribution of strain energy three-dimensionally related in the region close to crack is obtained. However, at the most part of the plate is "undisturbed state" where strain energy has constant value [4].

According to the Griffith theory it is assumed that cracks exist or can be initiated in a solid body when tensile stresses overpass some limiting (critical) value, or when the strain energy release rate is higher then the rate of the energy gained by forming of crack new free surfaces [25]. Crack is considered as a elliptical hole, where one of semi axes is close to zero, and ellipse is degenerating to a straight slit [9], [25].

Square plate  $100 \times 100$  mm, and 10 mm thick, loaded with tensile forces in  $y$  direction is taken as an example for analyzing stress state and deformation energy (strain energy) state. Elliptical hole at the middle of the plate is taken as model of Griffith crack [25]. Elliptical crack presented on Fig. 1 has semi-major axis  $a = 5$  mm and semi-minor axis  $b = 0.5$  mm. As material of the plate is taken polyester Palatal P-6 with Young's elasticity modulus  $E = 4460$  N/mm<sup>2</sup> and Poisson's ratio  $\nu = 0.38$ .

Cartesian coordinates  $x$ ,  $y$  and  $z$  with origin in the middle of the plate are used. So, coordinate  $x$  is varying between  $-50$  mm and  $+50$  mm,  $y$  is varying between  $-50$  mm and  $+50$  mm, and  $z$  is varying from  $-5$  mm and up to  $+5$  mm. Remote load is regularly distributed on the edge side of the plate and it has value  $q = 1$  N/mm<sup>2</sup>. Direction of loading force is in  $y$  - direction and it is perpendicular to the semi-major axis of the elliptical crack. Scheme of the plate with crack and loading is presented on Fig. 1.

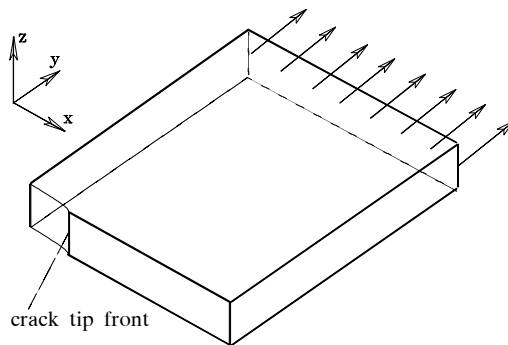


Fig. 1. Scheme of the plate with crack and loading

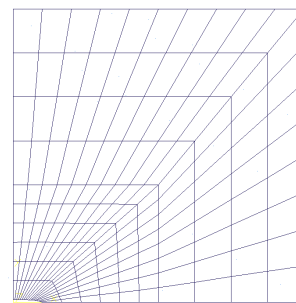


Fig. 2. Three-dimensional mesh of finite elements

## 2. STRESS DISTRIBUTION

Analytical methods like Williams polynomial method, and Westergaard's method are determining the stress components like two-dimensional stress state is valid even close to the crack tip, what is in disagreement with physical reality. It is possible to obtain analytical solution for stress state in a cracked plate by using Mushelishvili method [1], [5], [6], [7], [8], [9], and [10], but it is valid only in plates where two-dimensional stress state is omnipresent. Experimental experience shows evidently three-dimensional stress state on the crack tip [17], [18], [19], [20].

For determination of the stress tensor components in the vicinity of an elliptical crack the finite element method is used. Three-dimensional mesh of finite elements is generated, as it is presented on Fig. 2. It is generated manually in this way to simulate hyperbolic-elliptical coordinate system. Standard isoparametric, eight node brick elements are employed, precluding any erroneous to the imposition of an incorrect singularity [15].

By taking selected sections and directions it is determined distribution of normal and shear stresses for  $x$ ,  $y$  and  $z$ -axes in the selected points of the plate. Stress distribution for plane  $z = 0$  or the middle plane of the plate is determined.

Under given loading conditions, crack has tendency to increase semi-minor axis  $b$ , and to decrease semi-major axis  $a$ , of elliptical contour, or by common words to increase opening.

Stress components  $\sigma_x$ ,  $\sigma_y$ ,  $\sigma_z$ ,  $\tau_{xy}$ ,  $\tau_{yz}$ , and  $\tau_{zx}$ , at middle plane  $z = 0$  of the plate, in the region close to crack, are presented in Figures 3, 4, 5, 6, 7, and 8.

Stress components  $\sigma_x$ ,  $\sigma_y$ ,  $\sigma_z$ ,  $\tau_{xy}$ ,  $\tau_{yz}$ , and  $\tau_{zx}$ , at plane section  $y = 0$  of the plate, in the region close to crack, are presented in Figures 9, 10, 11, 12, 13, and 14. Previous two section planes are perpendicular to each other. Hence, stress components have equal values in direction  $y = 0$ ,  $z = 0$ .

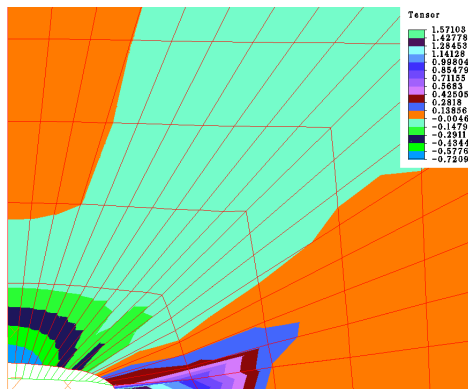


Fig. 3. Distribution of  $\sigma_x$  stress at middle plane  $z = 0$  of the plate.

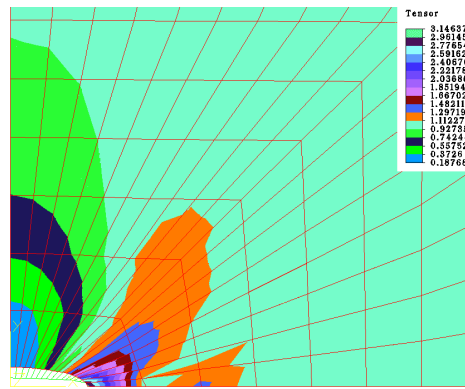


Fig. 4. Distribution of  $\sigma_y$  stress at middle plane  $z = 0$  of the plate.

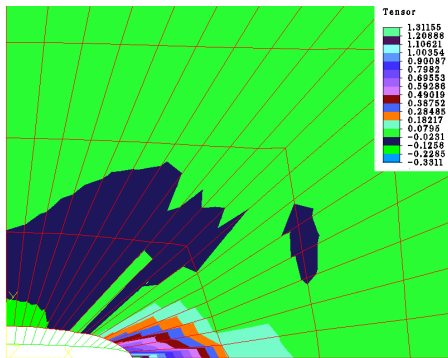


Fig. 5. Distribution of  $\sigma_z$  stress at middle plane  $z = 0$  of the plate.

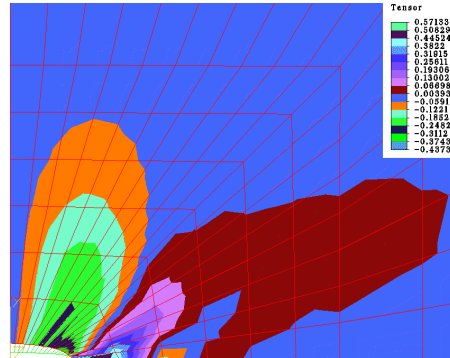


Fig. 6. Distribution of  $\tau_{xy}$  stress at middle plane  $z = 0$  of the plate.

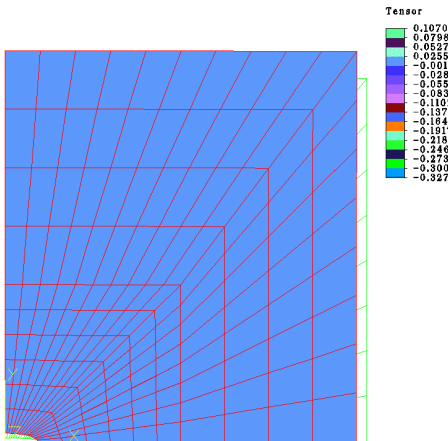


Fig. 7. Distribution of  $\tau_{yz}$  stress at middle plane  $z = 0$  of the plate.

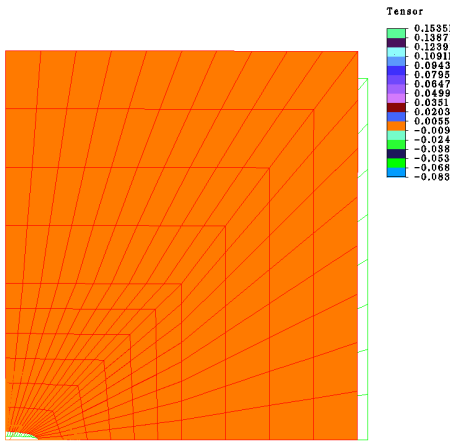


Fig. 8. Distribution of  $\tau_{zx}$  stress at middle plane  $z = 0$  of the plate.

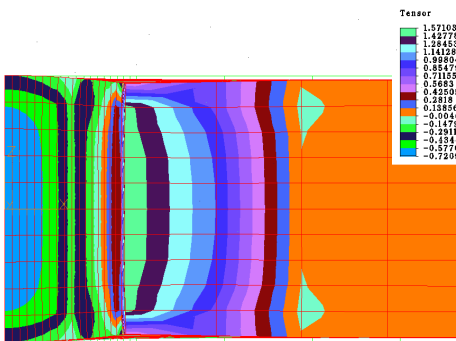


Fig. 9. Distribution of  $\sigma_x$  stress at plane section  $y = 0$  of the plate.

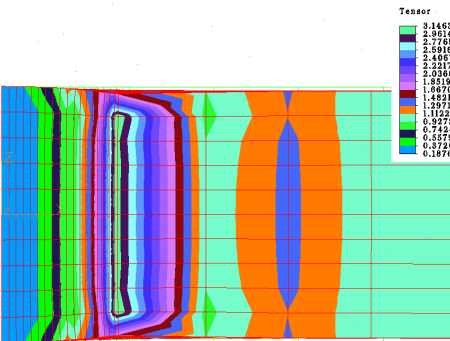


Fig. 10. Distribution of  $\sigma_y$  stress at plane section  $y = 0$  of the plate.

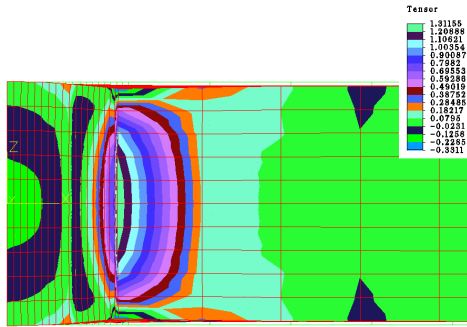


Fig. 11. Distribution of  $\sigma_z$  stress at plane section  $y = 0$  of the plate.

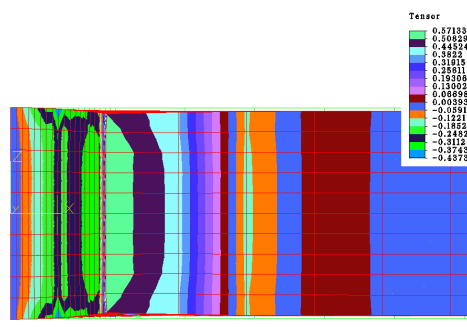


Fig. 12. Distribution of  $\tau_{xy}$  stress at plane section  $y = 0$  of the plate.

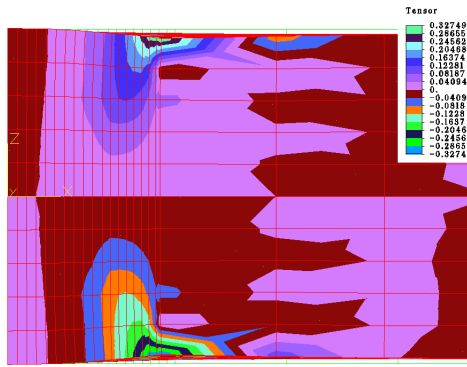


Fig. 13. Distribution of  $\tau_{yz}$  stress at plane section  $y = 0$  of the plate.

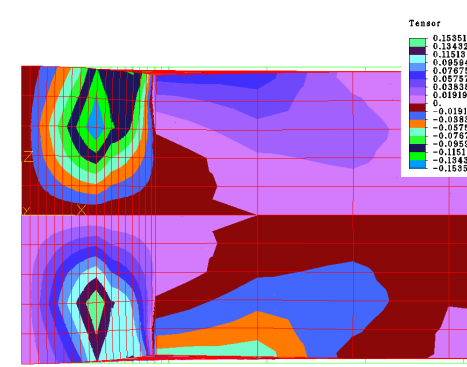


Fig. 14. Distribution of  $\tau_{zx}$  stress at plane section  $y = 0$  of the plate.

Diagrams of the stress components  $\sigma_x$ ,  $\sigma_y$ ,  $\sigma_z$ ,  $\tau_{xy}$ ,  $\tau_{yz}$ , and  $\tau_{zx}$ , for  $y = 0$  and  $z = 0$  are presented in Fig. 15, for  $y = 0$  and  $z = 2$  mm are presented in Fig. 16, for  $y = 0$  and  $z = 4$  mm are presented in Fig. 17, for  $x = 0$  and  $z = 0$  are presented in Fig. 18, for  $x = 4.5$  mm and  $z = 0$  are presented in Fig. 19, and for  $x = 7.028$  mm and  $z = 0$  are presented in Fig. 20. It is visible on Fig. 15, 16, and 17 that the highest values of  $\sigma_x$ ,  $\sigma_y$ ,  $\sigma_z$  and  $\tau_{xy}$  are on the crack tip front, and that  $\tau_{xy}$  changes sign on about one plate thickness from the crack tip. For direction  $x = 0$  and  $z = 0$  in Fig. 18 is visible that  $\sigma_x$ , and  $\sigma_z$  have sign minus in the region close to the crack edge up to 0.7 of the plate thickness for  $\sigma_x$ , and 0.5 of the plate thickness for  $\sigma_z$ . Stress component  $\sigma_y$  has increasing value from zero at the edge of crack up to value 1 N/mm<sup>2</sup> on distance 2.5 plate thickness from the crack edge. Stresses  $\sigma_x$ ,  $\sigma_z$  and  $\tau_{xy}$  are changing sign at the region in front of crack, as it is visible in Fig. 19 and Fig. 20.

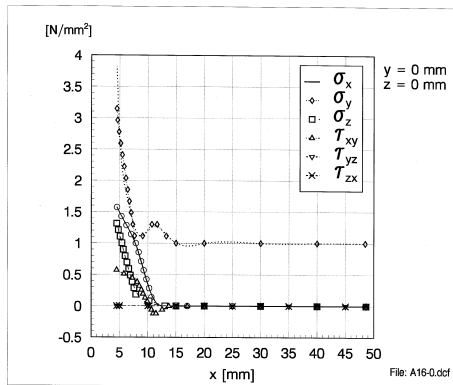


Fig. 15. Distribution of the stress components for  $y = 0$  and  $z = 0$ .

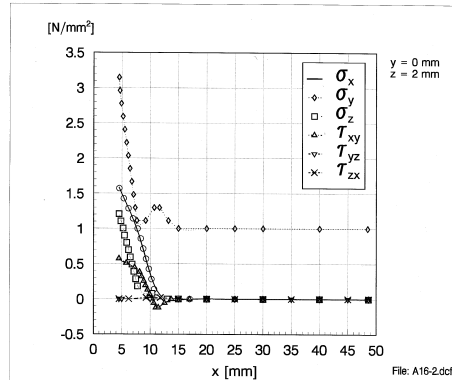


Fig. 16. Distribution of the stress components for  $y = 0$  and  $z = 2$  mm.

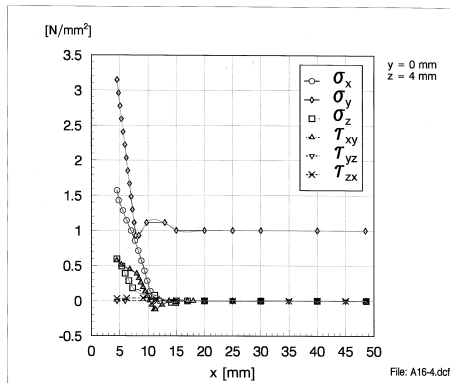


Fig. 17. Distribution of the stress components for  $y = 0$  and  $z = 4$  mm.

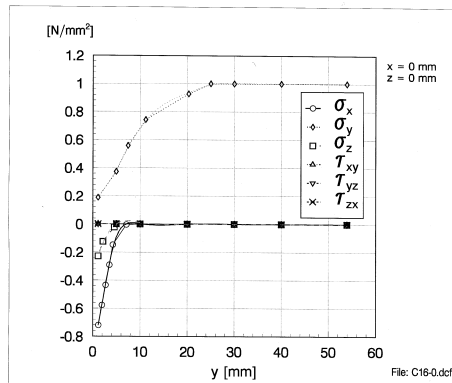


Fig. 18. Distribution of the stress components for  $x = 0$  and  $z = 0$ .

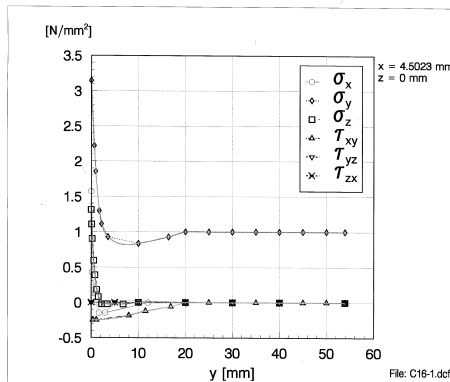


Fig. 19. Distribution of the stress for  $x = 4.5$  mm and  $z = 0$ .

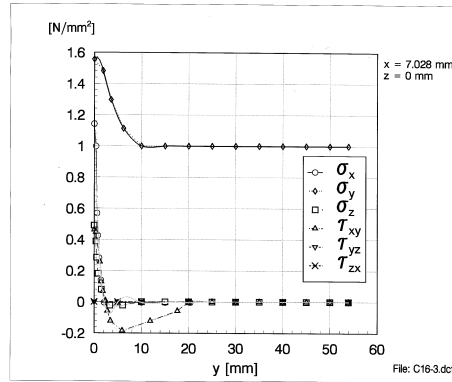


Fig. 20. Distribution of the stress components for  $x = 7.028$  mm and  $z = 0$ .

### 3. DISTRIBUTION OF THE DEFORMATION (STRAIN) ENERGY

When the elastic body is loaded, the work done by the applied forces is stored as a form of potential energy, which is frequently referred to as "strain energy" or, "elastic energy", or "deformation energy". If the body contains a crack, and that crack grows by a small amount under the applied loading conditions, the deformation energy stored in the body will be changed.

Specific deformation (strain) energy is calculated by using data from diagrams of stress tensor components presented on previous figures (see Fig.15 - 20), where interpolation and smoothing of stress function is previously done. For calculation of strain energy in selected characteristic directions FORTRAN program named "Defen" is created. Expression (1) well known in theory of elasticity [4], [11], [15], [27] is used.

$$A'_{def} = \frac{1}{2 \cdot E} [(\sigma_x^2 + \sigma_y^2 + \sigma_z^2) - 2 \cdot \nu(\sigma_x \sigma_y + \sigma_x \sigma_z + \sigma_y \sigma_z) + 2 \cdot (1 + \nu)(\tau_{xy}^2 + \tau_{xz}^2 + \tau_{yz}^2)] \quad (1)$$

Diagram of specific deformation energy (energy of elastic deformation per unit of volume) for direction  $y = 0, z = 0$  is presented in Fig. 21. Diagrams of specific deformation energy for directions  $x = 0, z = 0$ , and  $z = 0, x = 2.3, 4.5, 10.76$  are presented in Fig. 22, 23, 24, 25 respectively.

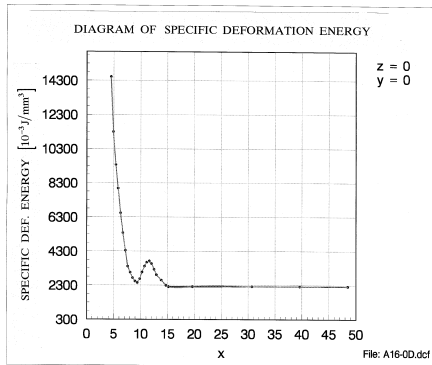


Fig. 21. Distribution of specific deformation (strain) energy for direction  $y = 0, z = 0$ .

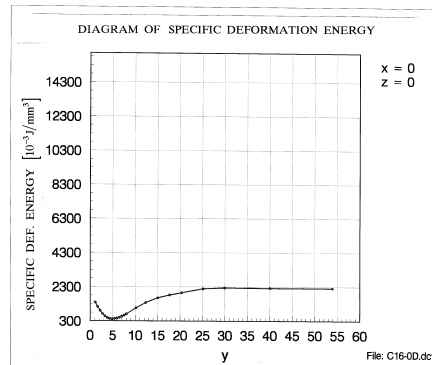


Fig. 22. Distribution of specific deformation (strain) energy for direction  $x = 0, z = 0$ .

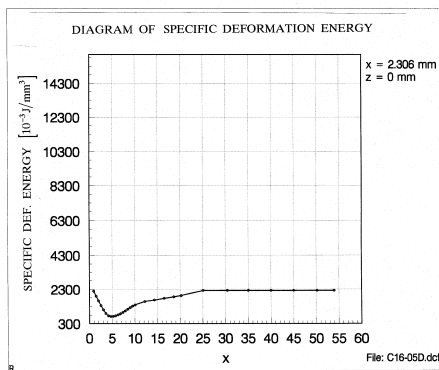


Fig. 23. Distribution of specific deformation energy for direction  $z = 0, x = 2.3$  mm.

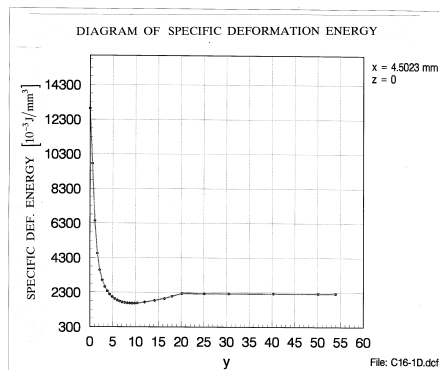


Fig. 24. Distribution of specific deformation energy for direction  $z = 0, x = 4.5$  mm.

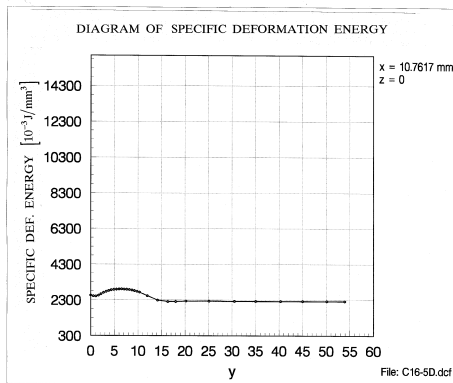


Fig. 25. Diagram of specific deformation energy for direction  $z = 0$ ,  $x = 10.76$  mm.

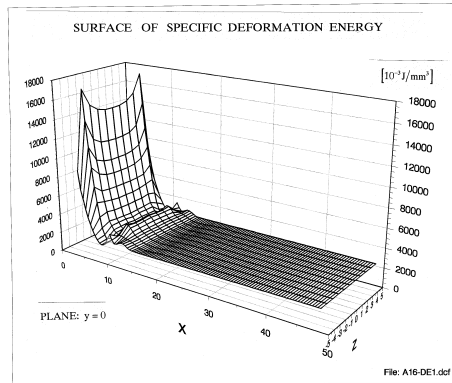


Fig. 26. Reconstructed surface of the specific deformation (strain) energy  $F = F(x,z)$  for plane  $y = 0$ .

By using data from diagrams of the specific deformation energy for various directions and by gridding, and smoothing the surfaces which are presenting distribution of specific deformation energy in planes  $z = 0$ ,  $F = F(x,y)$ , and  $y = 0$ ,  $F = F(x,z)$  are reconstructed. Surface of the specific deformation energy  $F = F(x,z)$  for plane  $y = 0$  is presented in Fig. 26.

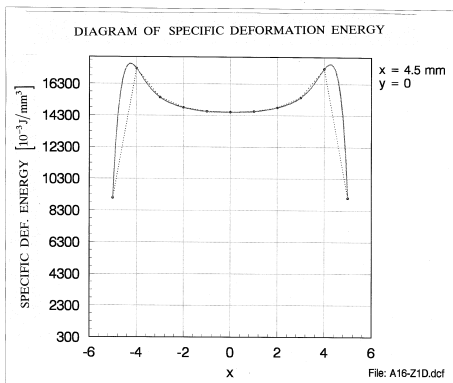


Fig. 27. Diagram of specific deformation energy at the crack tip front  $x = 4.5$  mm,  $y = 0$ .

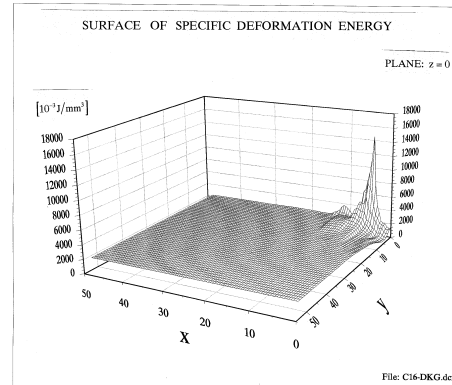


Fig. 28. Reconstructed surface of the specific deformation (strain) energy  $F = F(x,z)$  for plane  $z = 0$ .

It is visible that peaks of the deformation energy are on the crack front. Specific deformation energy is  $A'_{def} = 2230 \cdot 10^{-3} \text{ J/mm}^3$  at the distances higher than one plate thickness, and it is distance of undisturbed area. Diagram of specific deformation energy at the crack tip front  $x = 4.5$  mm,  $y = 0$  is presented in Fig. 27. The higher value of deformation energy is close to the plate, surfaces  $z = \pm 5$  mm, and it is  $A'_{def} = 17261.2 \cdot 10^{-3} \text{ J/mm}^3$  for  $z = \pm 4$  mm. From that values deformation energy is decreasing by parabolic function, and when we are going to the middle of the plate, it has value  $A'_{def} = 14517.6 \cdot 10^{-3} \text{ J/mm}^3$  for  $z = 0$ . It is visible on Fig. 28 that distribution of

strain energy resulted with high value of energy in front of crack tip, where the peak of energy stored in material exists. It is visible on Fig. 26 as well as on Fig. 27 that specific deformation (strain) energy is increasing from middle plane  $z = 0$  to front and back free surface of the plate, and that peaks of energy are close to free surfaces off the plate. This is observed only in region close to the crack front, up to distance of about 0.25 of plate thickness, from the crack front. This results are consistent with results of Sih G. C., Lee Y. D., [23] and their comment: "The inability of the elasticity theory to account for surface effects were not recognized and frequently left unexplained with the impression that they could be attributed to numerical inaccuracies". (Compare Fig. 26 and 27 with Fig. 11 in reference [23]). "The volume energy in Fig. 11 [23] at  $z \approx 0.233$  cm became even higher than at the mid-plane  $z = 0$ . This is contrary to physical intuition where the largest volume energy density should occur inside the plate, not near the surface. The success of this investigation lies not only in completing the three-dimensional finite element analysis but even more important is in understanding the near boundary behaviour of the elasticity solution that may not agree with physical intuition because it neglects the interaction of surface and volume effects [23]".

Values of deformation energy normalized to general level of deformation energy  $A'_{\text{def}} = 2230 \cdot 10^{-3} \text{ J/mm}^3$  and with normalized coordinates  $\bar{z}$  are given in Tab. 1.

Tab. 1. Specific deformation energy and normalized specific deformation energy at the crack tip front  $x = 4.5 \text{ mm}$ ,  $y = 0$

$\bar{z}$	Specific def. energy $A'_{\text{def}} [10^{-3} \text{ J/mm}^3]$	Normalized specific def. energy $\bar{A}'_{\text{def}}$
0.8	17261.2	7.74
0.6	15446.2	6.93
0.4	14801	6.64
0.2	14558.1	6.53
0.0	14517.6	6.51

Surface of the specific deformation energy  $F = F(x,y)$  for plane  $z = 0$  is presented on Fig. 28. It is visible in Fig. 28 that redistribution of deformation energy resulted with high energy on crack front, where is peak of the "mountain of energy". On the other side there is valley, with energy level lower than general (or global) energy level  $\bar{A}'_{\text{def}} = 1$ . The bottom of the valley has  $\bar{A}'_{\text{def}} = 0.185$ .

Depression of energy level is up to three plate thickness from the crack edge in direction of  $y$ -axis, as it is presented by diagram in Fig. 22.

It is clear that each material has (limiting or critical) energy level that observed material could tolerate without breaking of inter-atomic or inter-molecular bonds. That means, crack will not propagate if critical energy level is not overpassed. By using experimental procedure it is possible to determine critical energy level (CEL) for every material, and for all typical general stress states [19], [20].

Value of CEL can be used as criteria in determination of strength of materials and constructions to the process of crack development. Critical level of specific deformation energy is also important inherent characteristic of material.

## 4. COEFFICIENT OF ENERGY REDISTRIBUTION

If we establish ratio of peak value of specific deformation energy on the crack front against general value of specific deformation (strain) energy, this value could be named "coefficient of energy increasing":

$$C_I = \frac{A'_{\text{def}(P)}}{A'_{\text{def}(G)}} \quad (2)$$

where:

$A'_{\text{def}(P)}$  - is peak value of specific deformation energy, and  $A'_{\text{def}(G)}$  - is general value of specific deformation energy.

On the other side at the region of valley, energy is decreasing under the general level. There, relation between bottom value of energy and general energy level could be named "coefficient of energy decreasing":

$$C_D = \frac{A'_{\text{def}(B)}}{A'_{\text{def}(G)}} \quad (3)$$

where:  $A'_{\text{def}(B)}$  - is bottom value of specific deformation energy.

Relation between coefficient of energy increasing  $C_I$ , and coefficient of energy decreasing  $C_D$  gives third coefficient which could be named coefficient of energy redistribution  $C_R$ .

$$C_R = \frac{C_I}{C_D} \quad (4)$$

It is clear that coefficient of energy redistribution depends on crack geometry (relations between crack length, thickness of the plate, radius of the curvature on the crack tip, shape of the crack etc.), and it depends also on general stress state at the surrounding of the crack. Higher value of coefficient of energy redistribution means that concentration of energy at the crack tip is higher.

By using simple experiment can be determined coefficients  $C_I$ ,  $C_D$  and  $C_R$  for different crack parameters as useful tool for engineers.

## 5. LOCAL EFFECT OF THE CRACK

Analysis in this work shows that influence of the crack on the general stress state and energy state is local, and in the presented example local effect takes place up to one plate thickness from the crack tip. In other direction perpendicularly to crack length decreasing of energy happens up to three plate-thickness from the crack. On Fig. 15, 16, 17, 18, 19, 20, is visible that changing of stresses takes effect only in region of crack. Evidently that phenomenon of crack results at local changing of stress state, and local distribution of the specific deformation energy, at the region close to the crack.

General stress state in plate can be described by using well-known analytical solutions for plane stress state, generalized plane stress state and bending of plates [4], [27]. Meanwhile, at the region of crack exist three-dimensional stress state and three-dimensional distribution of specific deformation energy.

It would be the next step to introduce function of local three-dimensional stress redistribution  $\mathbf{D}_S$ , and function of local three-dimensional specific deformation energy redistribution  $\mathbf{D}_E$ .

Local function depends on three coordinates:

$$\mathbf{D}_E = \mathbf{D}_E(x, y, z) \quad (5)$$

So, distribution of specific deformation energy is:

$$\mathbf{A}'_{\text{def}} = \mathbf{D}_E(x, y, z) \cdot \mathbf{A}'_{\text{def R}} \quad (6)$$

Where  $\mathbf{A}'_{\text{def R}}$  - is general value of specific deformation energy, when crack does not exist.

Function  $\mathbf{D}_E(x, y, z)$  is undimensional:

$$\mathbf{D}_E(x, y, z) = \frac{\mathbf{A}'_{\text{def}}}{\mathbf{A}'_{\text{def R}}} \quad (7)$$

and it gives local distribution of deformation energy.

## 6. CONCLUSIONS

This paper presents stress state at the surrounding of an elliptical hole in elastic plate. From the diagrams of the stress components is visible that stress state is three-dimensional close to the crack. Normal stress  $\sigma_z$  is different than zero on distance up to three quarters of the plate thickness from the crack front at the direction of crack propagation and up to half of the plate thickness at the direction perpendicular to crack. It is also visible that stresses  $\sigma_x$ ,  $\sigma_y$ ,  $\sigma_z$  are depending on coordinate  $z$  up to one plate thickness from the crack front at the crack direction. Specific deformation energy is calculated at second step, and at the third step surfaces which are presenting distribution of the specific deformation energy are reconstructed. From these diagrams and surfaces which are presenting specific deformation energy is visible that crack is initiating redistribution of the deformation energy at the surrounding. Deformation energy is increasing up to one plate thickness in front of the crack tip at the direction of the crack, and decreasing up to three plate-thickness at direction perpendicular to the middle of the crack. Reconstructed specific energy surfaces are presenting visually, how crack influence deformation energy distribution at the plane stressed plate. Regions of the plate further from the crack remind undisturbed and deformation energy is clearly constant. Also, stress state on distance further than one plate thickness is evidently two-dimensional, and stresses are independent of thickness coordinate. This gives us opportunity to draw conclusion that influence of the crack is evidently local and the rest of the plate stays "undisturbed". This analysis is suggesting that analytical solutions should be locally three-dimensional.

Introduction of three-dimensional function that is presenting disturbing influence of the crack to stress state and distribution of deformation energy of the plate, could be appropriate direction to look forward.

**Acknowledgment.** *This research supported by Science Ministry of Serbia, grant number 04M03A through Mathematical Institute SANU, Belgrade. The author is grateful to Professor Dr. Katica Hedrih for her valuable suggestions.*

## REFERENCES

1. England A., (1971), *Complex variable Methods in Elasticity*, London.
2. Gdoutos E. E., *Fracture Mechanics*, Kluwer Academic Publishers, Dordrecht, 1993
3. Gdoutos E. E., *Problems of mixed mode crack propagation*, Martinus Nijhoff Publishers, Kluwer Academic Publishers, The Hague, 1984
4. Hedrih K., (1988), *Izabrana poglavlja Teorije elastičnosti*, Mašinski fakultet, Niš
5. Hedrih K., Jecić S., Jovanović D., (1990), *Glavni naponi u tačkama konture eliptično-prstenaste ploče ravno napregnute parovima koncentrisanih sila*, Mašinstvo br. 39, Beograd
6. Hedrih K., Jovanović D., (1990), *Primena funkcije kompleksne promenljive i konformnog preslikavanja za određivanje eliptično-hiperboličkih koordinata tenzora napona ravno napregnutih ploča*, XIX Jugoslovenski kongres teorijske i primenjene mehanike, Ohrid
7. Hedrih K., Jovanović D., *The stress state of the elliptical-annular plate by the complex variable function and conformal mapping method*, 15 str., 73-87, časopis, Teorijska i primenjena mehanika, br. 17, Jugoslovensko društvo za mehaniku, Beograd, 1991.
8. Hedrih K., Jovanović D., *The strain state of the elliptical - annular plate by the complex variable function and conformal mapping method*, 17 str., 29-45, časopis, Teorijska i primenjena mehanika, br. 21, Jugoslovensko društvo za mehaniku, Beograd, 1995.
9. Hedrih K., Jovanović D., *Stress state around elliptical cracks in elastic plates*, International minisymposium MF Recent Advances in Fracture and Damage Mechanics, Zbornik radova, Str. 153-157, YUCTAM Vrnjačka Banja, 1997
10. Jovanović D., (1990), *Primena metode fotoelastičnosti za ispitivanje naponskog stanja eliptično-prstenaste ploče opterećene koncentrisanim silama*, XIX Jugoslovenski kongres teorijske i primenjene mehanike, Ohrid
11. Kojić M., (1975), *Teorija elastičnosti*, Mašinski fakultet, Kragujevac
12. Love A.E.H., (1952), *A Treatise on Mathematical Theory of Elasticity*, Cambridge and University Press, Cambridge
13. Milne - Thompson L. M., (1960), *Plane elastic Systems*, Gottingen-Heidelberg, Springer, Berlin
14. Muskhelishvili N.I., (1953), *Some Basic problems of the Mathematical Theory of Elasticity*, P. Noordhof LTD., Groningen - Holland.
15. Parsons I. D., Hall J. F., Rosakis A. J., *A Finite Element Investigation of the Elastostatic State Near a Three Dimensional Edge Crack*, SM Report 86-29, Division of Engineering and Applied Science, California Institute of Technology, Pasadena, California, 1986
16. Rašković D., (1985), *Teorija elastičnosti*, Naučna knjiga, Beograd.
17. Pindera J. T., *Three-Dimensional Stress Analysis of Composite Structures Using Isodyne Techniques*, Polymer Composites, Vol. 10, No. 5, 270-284, October 1989
18. Pindera J. T., and Wen B., *Isodyne Evaluation of Three-Dimensional Stresses in Standard Compact Specimen*, SEM Spring Conference on Experimental Mechanics, Proceedings, 895-902, June, Milwaukee, Wisconsin, 1991
19. Pindera J. T., Josepson J. and Jovanović D.B., *Electronic Techniques in Isodyne Stress Analysis: Part 1. Basic Relations*, Experimental Mechanics, Vol. 37, No. 1, 33-38, March 1997
20. Pindera J. T., Josepson J. and Jovanović D.B., *Electronic Techniques in Isodyne Stress Analysis: Part 2. Illustrating Studies and Discussion*, Experimental Mechanics, Vol. 37, No. 2, 106-110, June 1997
21. Sedmak S. *Uvod u mehaniku loma i konstruisanje sigurnošću od loma*, monografija, Smederevska Palanka, Goša-TMF Beograd, 1980
22. Sih G. C., *Mechanics of Fracture Initiation and Propagation*, Kluwer Academic Publishers, Dordrecht, 1990
23. Sih G. C., Lee Y. D., *Review of Triaxial Crack Border Stress and Energy Behavior*, Theoretical and Applied Fracture Mechanics, No. 12, pp. 1-17, Elsevier Science Publishers, B. V., 1989
24. Shedon J. S. and Very D. S., (1958), *The Classical Theory of Elasticity*, Hand-Buch der Physik, S. Fluge, Band VI, Springer Verlag
25. Sneddon, I. N., Lowengrub, M., *Crack Problems in the Classical Theory of Elasticity*, John Wiley & Sons, Inc., New York, 1969
26. Sokolnikoff I. S., (1956), *Mathematical Theory of Elasticity*, McGraw Hill Book Company, London.
27. Timoshenko S. P. and Goodier J. N., (1951), *Theory of Elasticity*, New York
28. Theocaris P. S., *The Minimum Elastic Strain Energy Criterion for Mode I and II Fractures*, Proc. of Symp. on Absorbed Spec. Energy / Strain Energy Density Criterion, pp. 17-32, Budapest, Hungary, 1980

**STANJE NAPONA I RASPORED ENERGIJE DEFORMACIJE  
(DILATACIJE) ISPRED VRHA PRSLINE  
U PLOČI IZLOŽENOJ ZATEZANJU**

**Dragan B. Jovanović**

*U ovom radu je korišćen trodimenzionalni model ploče sa eliptičnom prslinom za analizu stanja napona i energije deformacije. Pretpostavljeno je dejstvo zatežućih sila u pravcu upravnom na ravan prsline i ravno stanje napona kao opšte (u području udaljenom od prsline). trodimenzionalno stanje napona Ustanovljeno je korišćenjem metode konačnih elemenata da u oblasti prsline vlada trodimenzionalno stanje napona. Promena komponenti tenzora napona je u funkciji koordinate upravne na srednju ravan ploče i  $\sigma_z$  je različito od nule u oblasti neposredno oko prsline.*

*U radu su analizirani dobijeni rezultati o rasporedu napona i rasporedu deformacione energije i dobijeni su zaključci o trodimenzionalnom stanju napona i trodimenzionalnom rasporedu energije u neposrednoj okolini linije fronta prsline.*

*Ključne reči: prslina, stanje napona, specifična energija deformacije, rekonstrukcija površina energije*